Development 140, 2587-2596 (2013) doi:10.1242/dev.089052

Fibronectin mediates mesendodermal cell fate decisions

Paul Cheng[1,2,*], Peter Andersen[1,3,*], David Hassel[4,6,7], Bogac L. Kaynak[1,‡], Pattraranee Limphong[3], Lonny Juergensen[7], Chulan Kwon[1,3,§] and Deepak Srivastava[1,4,5,6,§]

SUMMARY

Non-cell-autonomous signals often play crucial roles in cell fate decisions during animal development. Reciprocal signaling between endoderm and mesoderm is vital for embryonic development, yet the key signals and mechanisms remain unclear. Here, we show that endodermal cells efficiently promote the emergence of mesodermal cells in the neighboring population through signals containing an essential short-range component. The endoderm-mesoderm interaction promoted precardiac mesoderm formation in mouse embryonic stem cells and involved endodermal production of fibronectin. *In vivo*, fibronectin deficiency resulted in a dramatic reduction of mesoderm accompanied by endodermal expansion in zebrafish embryos. This event was mediated by regulation of Wnt signaling in mesodermal cells through activation of integrin-β1. Our findings highlight the importance of the extracellular matrix in mediating short-range signals and reveal a novel function of endoderm, involving fibronectin and its downstream signaling cascades, in promoting the emergence of mesoderm.

KEY WORDS: Fibronectin, Endoderm, Mesoderm, Integrin-β1, Wnt

INTRODUCTION

Cells that contribute to the heart arise from distinct pools of mesodermal progenitors during embryonic development and are typically characterized by expression of specific transcription factors (Srivastava, 2006). Several lineage-tracing studies have demonstrated the origin and location of distinct populations of precardiac mesodermal cells (Buckingham et al., 2005). The specification, fate and expansion of cardiac mesodermal progenitors are controlled by diffusible morphogens, such as Wnt, Nodal, BMP and FGF (Murry and Keller, 2008; Mercola et al., 2011). Such non-cell-autonomous signals from early endoderm have long been implicated in the formation of cardiac progenitors (Schultheiss et al., 1995; Schultheiss and Lassar, 1997; Marvin et al., 2001; Ueno et al., 2007). Furthermore, the function of transcription factors, such as Gata4 and Sox17/18 in the endoderm, is required for appropriate cell-cell signaling (Liu et al., 2007; Holtzinger et al., 2010). However, the precise mechanisms by which endoderm-mesoderm communication occurs leading to the specification of precardiac mesoderm remain unclear.

The ability of embryonic stem (ES) cells to spontaneously differentiate into cardiomyocytes offers an opportunity to study non-cell-autonomous signals *in vitro*, as co-culturing ES cells with endoderm-like (End2) cells is known to enhance cardiac differentiation (Mummery et al., 2003; Rudy-Reil and Lough, 2004). Conversely, loss of the endodermal HMG-box transcription factor Sox17/18 in ES cell culture suppresses cardiomyogenesis non-cell-autonomously, but the suppression can be rescued by co-culturing ES cells with normal endodermal cells (Liu et al., 2007).

Here we investigated the mechanisms of endoderm-mediated differentiation of the cardiac lineage and found that endodermal cells promote precardiac mesoderm through signals containing a crucial short-range component involving the extracellular matrix protein fibronectin 1 (Fn1). Fn1 in turn activated β-catenin signaling through integrin-β1, and this signaling event biased cells, probably in conjunction with other secreted signals, toward the precardiac mesoderm fate.

MATERIALS AND METHODS

Cell culture and differentiation

Mouse ES (mES) cells were propagated in an undifferentiated state on gelatin-coated cell culture plastic (Nunc) in GMEM supplemented with 10% FBS, 0.1 mM non-essential amino acids, 2 mM GlutaMAX, 0.1 mM sodium pyruvate (Invitrogen), 0.1 mM 2-mercaptoethanol (Sigma-Aldrich) and 1500 U/ml leukemia inhibitory factor (LIF; Millipore). ES cells were passaged every 2-3 days with TrypLE Express (Invitrogen) with daily medium changes.

For co-culture experiments, ES cells and End2 cells were dissociated to single cells and plated on ultra-low attachment plastic surface (Corning) in IMDM/Ham's F12 (Cellgro) (3:1) supplemented with N2, B27, penicillin/streptomycin, 2 mM GlutaMAX, 0.05% BSA, 5 ng/ml L-ascorbic acid (Sigma-Aldrich) and α-monothioglycerol (MTG; Sigma-Aldrich) at a final density of 75,000 cells/ml.

For cardiac mesoderm induction, cells were propagated as described above (75,000 cells/ml) for 48 hours. Embryoid bodies (EBs) were collected and dissociated to single cells. Cells were replated on ultra-low attachment plastic surface as described above and induced for 40 hours with activin A (5 ng/ml), BMP4 (0.5 ng/ml) and VEGF (10 ng/ml) (R&D Systems).

For cardiac differentiation, GFP^+ cells from co-cultures were plated on gelatin-coated cell culture plastic (Nunc) in StemPro34 (Invitrogen) supplemented with 10 ng/ml L-ascorbic acid, penicillin/streptomycin, 2 mM GlutaMAX, FGF (20 ng/ml), FGF10 (50 ng/ml) and VEGF (10 ng/ml) (all from R&D Systems). Unbiased differentiation was achieved by growing EBs in 20% FBS in GMEM supplemented with 2 mM GlutaMAX and 0.1 mM non-essential amino acids.

$ES^{Bry\text{-}GFP}$ cells were a kind gift from G. Keller (McEwen Centre for Regenerative Medicine, Toronto, Canada). $ES^{Nkx2.5\text{-}GFP}$ cells were generated from the mouse E14 ES cell line carrying RP11-88L12/NKX2-5-Emerald

[1]Gladstone Institute of Cardiovascular Disease, San Francisco, CA 94158, USA. [2]Bioengineering, University of California San Francisco, San Francisco, CA 94158, USA. [3]Division of Cardiology and Institute for Cell Engineering, Johns Hopkins University School of Medicine, 720 Rutland Avenue, Baltimore, MD 21205, USA. [4]Roddenberry Center for Stem Cell Biology and Medicine at Gladstone, San Francisco, CA 94158, USA. [5]Department of Pediatrics, University of California San Francisco, San Francisco, CA 94158, USA. [6]Biochemistry and Biophysics, University of California San Francisco, San Francisco, CA 94158, USA. [7]Department of Internal Medicine III, University Hospital Heidelberg, Heidelberg 400 69120, Germany.

*These authors contributed equally to this work
‡Present address: Institute of Biotechnology, PL56, 00014 University of Helsinki, Finland
§Authors for correspondence (ckwon13@jhmi.edu; dsrivastava@gladstone.ucsf.edu)

Accepted 20 March 2013

GFP as described (Hsiao et al., 2008). The ES^{GFP} cell line is a variant of the E14 line that expresses GFP under control of the CMV/β-actin (CAG) promoter. All mES cells used in this study were E14 derivatives. Neural stem cells (NSCs) were obtained from ATCC. End2 cells were a kind gift from C. Mummery (Leiden University Medical Centre, Leiden, The Netherlands).

Luciferase assays

For TOP/FOP-flash luciferase assays, transfected mES cells were treated with 20 ng/ml Wnt3A, 2 μM BIO and/or anti-CD29 (Itgb1) (BD Biosciences) for 24 hours before analysis. TOP/FOP-flash luciferase constructs were kindly provided by Randall Moon (University of Washington, WA, USA).

Isolation of visceral endoderm and extra-embryonic ectoderm

Visceral endoderm or extra-embryonic ectoderm (ExE) was isolated by microdissection of 20 mouse embryos at embryonic day (E) 6.5. Endoderm or ExE was dissociated into single cells and co-cultured with $ES^{Bry\text{-}GFP}$ cells in a 1:10 ratio.

qRT-PCR

RNA was extracted with TRIzol (Invitrogen). Quantitative reverse transcription PCR (qRT-PCR) was performed using the Superscript III first-strand synthesis system (Invitrogen) followed by use of TaqMan probes on the ABI 7900HT real-time PCR system (Applied Biosystems) according to the manufacturer's protocols. Optimized primers from TaqMan gene expression arrays were used. Expression levels were normalized to that of *Gapdh*. All samples were run at least in triplicate. Real-time PCR data were normalized and standardized with SDS2.2 software (Applied Biosystems).

Flow cytometry and FACS analysis

Cells were dissociated and percentages of GFP^+ and $cTnT^+$ cells were analyzed using a FACSCalibur flow cytometer (BD Biosciences) and FlowJo software (TreeStar). For cTnT expression, cells were incubated with anti-cTnT antibody (Neomarkers) followed by incubation with secondary antibody conjugated with Alexa Fluor 647 (Invitrogen). For FACS, cells were dissociated as described above, resuspended in PBS containing 0.1% FBS, 20 mM Hepes and 1 mM EDTA, and sorted on a FACSAria I or II cell sorter (BD Biosciences). FACS analyses were performed on days indicated in the figures.

siRNA knockdown, antibody-targeted inhibition of integrin-β1 and fibronectin

For knockdown studies, ON-TARGET Smartpools of *fn1* siRNA, collagen Ia1, collagen IVa1, collagen IVa2, Sparc siRNA, scrambled siRNA (control) (Dharmacon) or Block-iT Alexa Fluor Red (Invitrogen) were used at 75 nM. End2 cells were transfected using Lipofectamine RNAiMAX (Invitrogen) 24 hours before co-culture experiments. For antibody inhibition studies, anti-CD29 (anti-integrin-β1, BD Biosciences) or anti-Fn1 (Developmental Studies Hybridoma Bank) was added from the start of the experiment at the concentrations described.

Embryo immunostaining

E6.75 embryo cryosections were stained with anti-Fn1, anti-collagen I, anti-collagen IV or anti-Sparc (Abcam), followed by incubation with secondary antibodies conjugated with Alexa Fluor 488 or 546 (Invitrogen).

Mouse extracellular matrix (ECM) PCR array

The ECM RT^2 Profiler PCR Array (PAMM-013) was obtained from SABiosciences. The following samples were used: (1) $ES^{CAG\text{-}GFP}$ cells; (2) $ES^{CAG\text{-}GFP}$ cells that had been differentiated with End2 cell co-culture for 2.5 days and sorted by FACS; (3) NSCs; (4) End2 cells from condition (2) that were negatively sorted by FACS to remove ES cells; and (5) End2 cells. RNA was extracted with TRIzol (Invitrogen). qRT-PCR was performed using the Superscript III first-strand synthesis system (Invitrogen). The ECM RT^2 Profiler PCR Array was run on the ABI 7900HT according to the manufacturer's instructions (Applied Biosystems). Data from conditions (4) and (5) were compared with data from conditions (1-3). Results were analyzed and visualized using software provided from the manufacturer with the arrays. ECM gene comparative expression data are given in supplementary material Table S1.

Western blotting

Cell lysate was resolved by SDS-PAGE and electroblotted onto PVDF membranes. The membranes were incubated with primary antibodies in 5% nonfat milk overnight at 4°C, and secondary antibodies for 1 hour at room temperature. Detection was by chemiluminescence (Amersham ECL, GE Healthcare Life Sciences).

Zebrafish studies

Zebrafish (*Danio rerio*) care and breeding were carried out as described (Westerfield, 1995). For *in vivo* knockdown studies in zebrafish, previously described morpholino antisense oligonucleotides against the translational start sites of zebrafish *fibronectin 1* (MO-*fn1*, 5′-TTTTTTCACA-GGTGCGATTGAACAC-3′) (Trinh and Stainier, 2004) and zebrafish *fibronectin 1b* (MO-*fn1b*, 5′-TACTGACTCACGGGTCATTTTCACC-3′) (Jülich et al., 2005) and a control scrambled non-targeting morpholino were injected individually (6-8 ng) or in combination into one-cell stage zebrafish embryos.

Whole-mount *in situ* hybridization of stage-matched zebrafish embryos was carried out as described (Fish et al., 2008). Embryos were staged before the procedure as described (Kimmel et al., 1995). Zebrafish *ntl* and *gsc* expression vectors used as templates for digoxigenin-labeled RNA antisense probe synthesis were kindly provided by D. Stainier (Max Planck Institute for Heart and Lung Research, Bad Nauheim, Germany).

Statistical analyses

The two-tailed Student's *t*-test, type II, was used for data analyses. $P<0.05$ was considered significant.

RESULTS

Endodermal cells promote the emergence of brachyury$^+$ mesoderm via a short-range signal

Since endoderm has an inductive role in cardiogenesis (Schultheiss et al., 1995; Mummery et al., 2003; Rudy-Reil and Lough, 2004), we investigated the range and nature of this inductive signal. Given the proximity of endoderm and nascent mesoderm during early development *in vivo* (Nijmeijer et al., 2009), we hypothesized that the induction of precardiac mesoderm involves close contact with endoderm. To test this, mouse ES (mES) cells were differentiated by aggregation with or without End2 cells, or in End2 cell-conditioned medium. After 8 days of differentiation, 65% of embryoid bodies (EBs) co-cultured with End2 cells had beating foci, compared with 25% or 20% when co-cultured with mES cells alone or in conditioned medium, respectively (Fig. 1A). Correspondingly, the number of cardiomyocytes, marked by the sarcomeric protein cardiac troponin T (cTnT; Tnnt2 – Mouse Genome Informatics), was fourfold greater in EBs formed with End2 cells, as quantified by fluorescence-activated cell sorting (FACS) (Fig. 1B). Furthermore, expression of the cardiac transcription factor gene *Nkx2.5* and the cardiac sarcomeric genes α-cardiac actin (*Actc1*) and myosin heavy chain 7 (*Myh7*) was significantly elevated upon co-aggregation with End2 cells (Fig. 1C), compared with mES cells cultured alone or in conditioned medium. Increasing the ratio of End2 cells to mES cells resulted in a dose-dependent increase in expression of *Actc1* and of the cardiac transcription factor gene *Hand2* (supplementary material Fig. S1A).

To test the relationship between cell-cell contact and mesoderm formation in cells exposed to the same medium, we mixed EBs formed from co-culture of mES cells stably expressing GFP ($mES^{CAG\text{-}GFP}$) and End2 cells, with EBs formed from unlabeled mES cells without End2 cells. After 8 days of differentiation in a mixed suspension culture, beating EBs were scored for fluorescence to determine the influence of End2 cells. The percentage of GFP^+ EBs that were beating was fivefold greater than for EBs cultured without End2 cells (supplementary material Fig. S1B). These

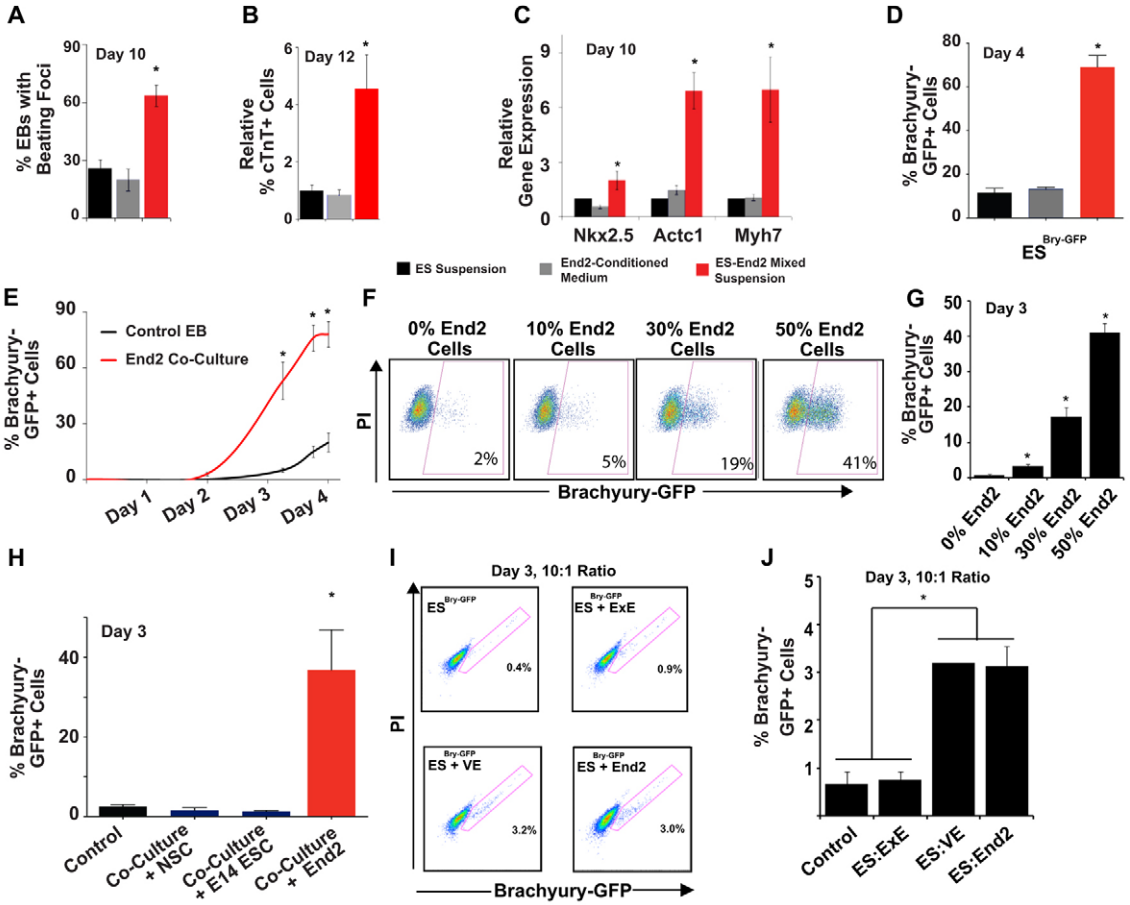

Fig. 1. Endoderm-like (End2) cells promote the emergence of mesoderm in ES cells through a short-range signal. (**A-C**) Co-aggregation of mouse ES (mES) cells with End2 cells during embryoid body (EB) differentiation resulted in increases in (A) the number of EBs with beating foci, (B) the percentage of cardiac troponin T (cTnT)$^+$ cells and (C) cardiac gene expression. Improvement in cardiac induction was not observed in EB differentiation with End2-conditioned medium. (**D**,**E**) Percentage of brachyury (Bry)-GFP$^+$ mesodermal cells in EBs differentiated with End2 cells or End2-conditioned medium. (**F**,**G**) FACS plot (F) and quantification (G) of Bry-GFP$^+$ cells at day 3 in EBs differentiated with increasing ratios of End2 cell co-culture. (**H**) Percentage of Bry-GFP$^+$ cells at day 3 in co-culture of mES cells with End2 cells, neural stem cells (NSCs) or other mES cells (E14 ESC). (**I**,**J**) FACS plot (I) and quantification (J) of Bry-GFP$^+$ cells at day 3 in co-culture with smaller numbers of End2 cells, visceral endoderm (VE) or extra-embryonic ectoderm (ExE) isolated from E6.5 mouse embryos at 10:1 ratio of mES cells:End2/VE/ExE. *P<0.05, n≥5 for all experiments. Error bars indicate s.e.m. of biological replicates.

experiments suggest that an important component of the inductive effect of End2 cells is being mediated by a short-range signal. End2 cells did not proliferate in EB suspension culture (supplementary material Fig. S1C), and treatment of End2 cells with mitomycin C to arrest cell division before co-culture did not affect their cardiogenic potency (data not shown).

One of the earliest lineage markers of mesodermal precursors is brachyury (Bry), a T-box-containing transcription factor expressed in the primitive streak/early mesoderm (Wilkinson et al., 1990; Kispert and Herrmann, 1994; Inman and Downs, 2006). To determine whether End2 cells affect the emergence of Bry$^+$ cells, we utilized an ES cell line with *GFP* knocked into the endogenous *Bry* locus (mES$^{Bry\text{-}GFP}$) (Fehling et al., 2003), and aggregated mES$^{Bry\text{-}GFP}$ cells with End2 cells (1:1) to form EBs in suspension. EBs co-aggregated with End2 cells showed an increased percentage of Bry$^+$ cells compared with control cells (Fig. 1D,E). In addition, the co-aggregation resulted in increased emergence of Bry$^+$ cells in a dose-dependent manner, suggesting an inductive role of the End2 cells at day 3 (Fig. 1E-G). No induction was observed when mES$^{Bry\text{-}GFP}$ cells were co-aggregated with ectodermal cells or other mES cells (Fig. 1H). The Bry-promoting effect appeared to involve an essential short-range component, as neither conditioned medium nor concentrated conditioned medium increased the percentage of Bry$^+$ cells (supplementary material Fig. S1D). To determine whether endoderm had a similar effect, mES$^{Bry\text{-}GFP}$ cells were co-aggregated at a 10:1 ratio with visceral endoderm or extra-embryonic ectoderm (ExE) cells isolated by manual dissection from E6.5 mouse embryos. Similar to End2 cells, the endodermal cells were able to induce Bry-GFP$^+$ cells from mES$^{Bry\text{-}GFP}$ cells, whereas ExE cells had no effect (Fig. 1I,J).

Bry transiently marks mesendoderm, and Bry$^+$ cells can give rise to a variety of different mesendodermal lineages (Hansson et al., 2009). By qPCR, we found that End2 cell-induced Bry-GFP$^+$ cells, sorted at day 4 of differentiation, expressed markedly higher levels of *Mesp1*, the earliest marker for cardiovascular progenitors (Fig. 2A), and of the well-established precardiac mesoderm markers *Kdr* and *Pdgfra* (Kitajima et al., 2000; Kattman et al., 2011), compared with Bry-GFP$^+$ cells isolated from normal ES cell differentiation (Fig. 2B). By contrast, the endodermal HMG-box transcription factor Sox17 was expressed at significantly

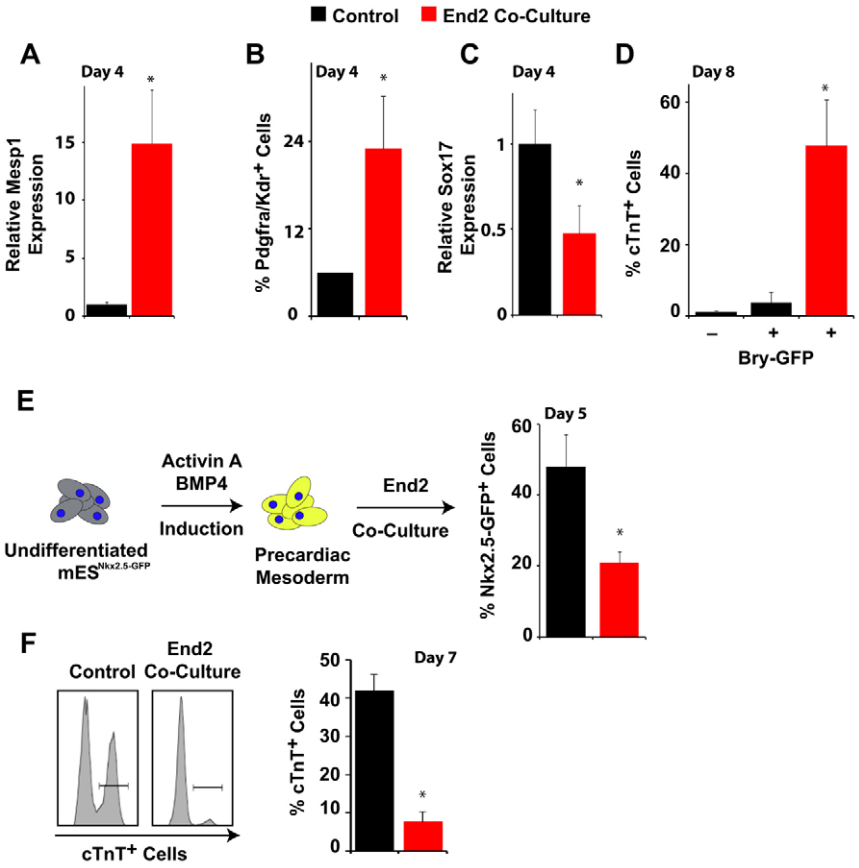

Fig. 2. End2-induced mesoderm is biased toward precardiac mesoderm. (**A**) qPCR analysis of relative *Mesp1* expression in Bry-GFP$^+$ cells isolated from mES$^{Bry\text{-}GFP}$ cells at day 4 with control or End2 cell co-culture. (**B**) Relative number of Kdr$^+$ Pdgfrα$^+$ cells among Bry-GFP$^+$ cells isolated from control or End2 co-culture. (**C**) Relative Sox17 expression in Bry-GFP$^+$ cells isolated at day 4 from mES$^{Bry\text{-}GFP}$ cells with control or End2 cell co-culture. (**D**) Percentage of cTnT$^+$ cells at day 8 from Bry-GFP$^+$ or Bry-GFP$^-$ cells isolated from control or End2 co-culture conditions. (**E**,**F**) Percentage of GFP$^+$ cells (E) or cTnT$^+$ cells (F) derived from mES$^{Nkx2.5\text{-}GFP}$ cells differentiated into precardiac mesoderm that was then co-cultured with End2 or control cells as illustrated. *P<0.05, n≥5. Error bars indicate s.e.m. of biological replicates.

lower levels compared with non-induced Bry-GFP$^+$ cells (Fig. 2C). To determine the fate of the End2 cell-induced Bry-GFP$^+$ cells, FACS-isolated Bry-GFP$^+$ cells at day 4 were replated and differentiated for 3 additional days in conditions that favor cardiac differentiation (Kattman et al., 2006). Under these conditions, End2 cell-induced Bry-GFP$^+$ cells formed a spontaneously contracting sheet of cardiomyocytes (supplementary material Movie 1) with 50% of the cells staining positive for cTnT (Fig. 2D), compared with less than 5% in the control Bry-GFP$^+$ cells, suggesting that the endoderm-induced signal favored precardiac mesoderm.

To determine if End2 cells further improve cardiac differentiation after formation of precardiac mesoderm, we examined whether End2 cells affect the progression of precardiac mesoderm to Nkx2.5$^+$ cardiac progenitors. Using an established combination of activin A and BMP4 (Kattman et al., 2006; Yang et al., 2008), we induced precardiac mesoderm (Bry$^+$ Mesp1$^+$) at day 4 of differentiation in mES$^{Nkx2.5\text{-}GFP}$ cells carrying a GFP reporter in the *Nkx2.5* locus (Hsiao et al., 2008), followed by co-culture with End2 cells. Interestingly, co-culture with End2 cells at this later stage inhibited the progression of Bry$^+$ Mesp1$^+$ precardiac mesoderm cells into Nkx2.5$^+$ progenitors and cardiomyocytes (Fig. 2E,F), suggesting that the inductive signal functions during a narrow window and does not act beyond precardiac mesoderm induction.

Fibronectin promotes the emergence of Bry$^+$ mesoderm

Our earlier experiments suggested that the mesoderm-promoting signal from endoderm might have an important short-range component. We hypothesized that, in addition to known diffusible proteins (Freund et al., 2008), this effect might be mediated via extracellular matrix (ECM) components secreted by the endoderm. To screen for ECM candidates responsible for the observed effect, we used ECM-specific gene expression arrays to compare End2 cells with mES cells or ectodermal cells. We identified nine ECM genes with transcripts that were highly enriched (>4-fold) in End2 cells (Fig. 3A). Of these genes, *Fn1*, *Sparc*, collagen Ia1 (*Col1a1*), collagen IVa1 (*Col4a1*) and collagen IVa2 (*Col4a2*) were temporally expressed around the egg cylinder and gastrulation stages in mice, according to published EST profiles.

We examined the expression of these five genes in E6.5 mouse embryos by immunofluorescent staining of the proteins, and found that they were spatially expressed in the endoderm, but not in the epiblast (Fig. 3B). To determine whether any of the candidate proteins were involved in promoting Bry$^+$ mesoderm, we used siRNA to knock down each candidate in End2 cells, and then co-cultured these End2 cells with mES$^{Bry\text{-}GFP}$ cells. Knockdown efficacies were confirmed by qPCR (supplementary material Fig. S2A). Knockdown of Fn1 reduced the formation of Bry-GFP$^+$ cells by 50%, whereas knockdown of Sparc, Col1a1, Col4a1 or Col4a2 had no effect (Fig. 3C). Similarly, blocking Fn1 activity by the addition of antibodies against extracellular Fn1 significantly reduced the formation of Bry-GFP$^+$ cells (supplementary material Fig. S2B). Likewise, we noted an End2 dose-dependent increase in Fn1 expression in our initial co-culture experiment (supplementary material Fig. S2C). Further analysis of EBs formed in the co-culture showed that Bry-GFP$^+$ cells generally emerged adjacent to fibronectin matrices (supplementary material Fig. S2D). These results suggested that Fn1 might be a key short-range signal that promotes mesoderm formation.

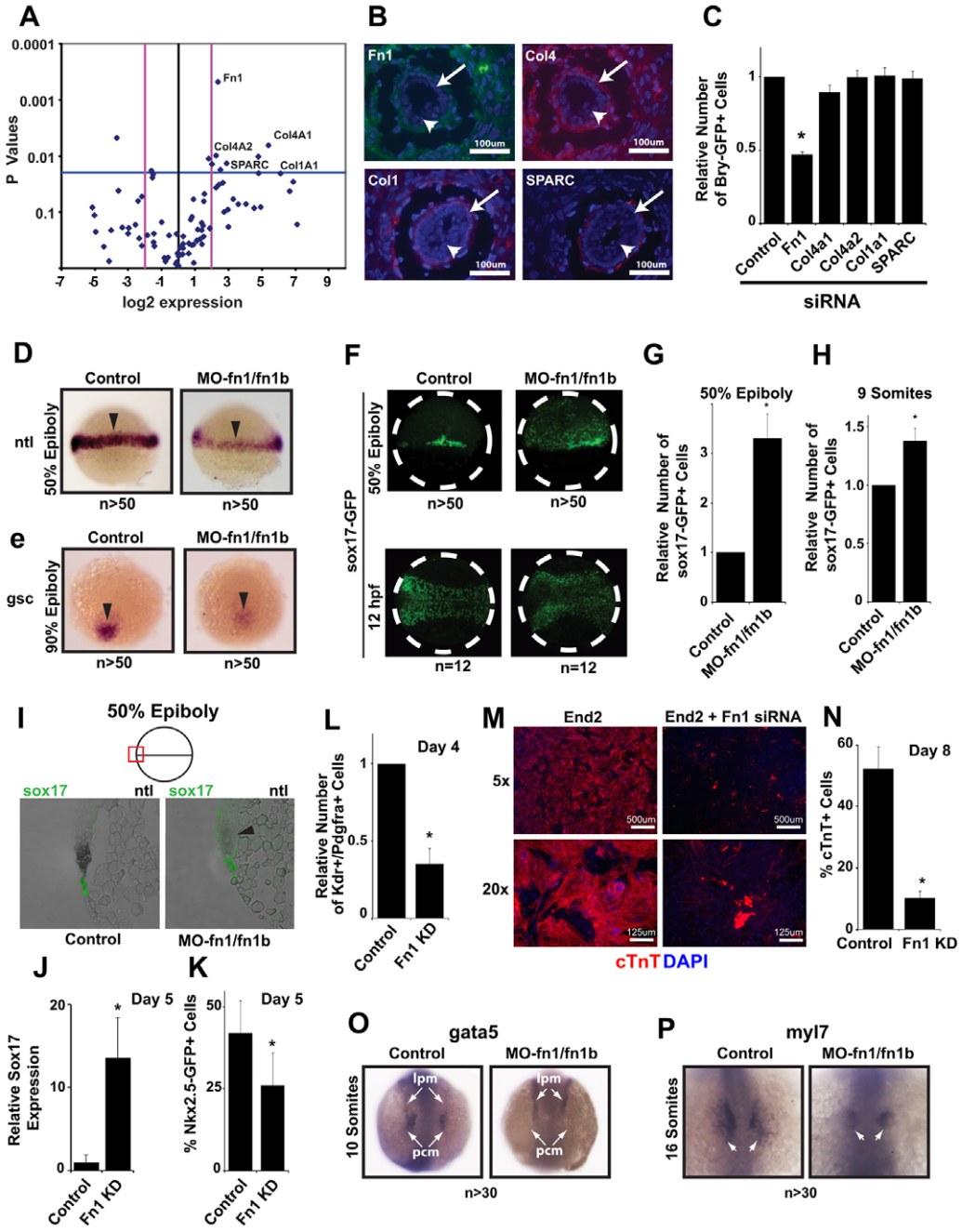

Fig. 3. Fibronectin promotes End2-mediated induction of mesoderm and precardiac mesoderm *in vitro* and *in vivo*. (**A**) Volcano plot of an ECM expression array comparing End2 versus control cells. (**B**) Transverse sections of E6.5 mouse immunostained for Fn1, Col4, Col1 or Sparc. Arrows indicate visceral endoderm and arrowheads indicate epiblast. (**C**) Bry-GFP^{+} cells induced by co-culturing mES$^{Bry\text{-}GFP}$ cells with End2 cells containing siRNA knockdown of Fn1, Col4a2, Col4a1, Col1a1 or Sparc. (**D**) *ntl* expression (arrowheads) examined by *in situ* hybridization in zebrafish embryos injected with control or *fn1/fn1b* morpholinos (MO-*fn1/1b*) at mid-gastrulation (50% epiboly; dorsolateral view, animal pole on top). (**E**) *gsc* expression (arrowheads) examined by *in situ* hybridization in zebrafish embryos injected with control or MO-*fn1/1b* at late gastrulation (90% epiboly; dorsal view, animal pole on top). (**F**) GFP expression in transgenic *sox17*-GFP zebrafish embryos injected with control or MO-*fn1/1b* at 50% epiboly (5.5 hpf; dorsal view, animal pole to the top) and at the 9-somite stage (12 hpf; dorsal view, anterior to the left). The dashed line indicates embryo border. (**G**) Relative number of *sox17*-GFP^{+} cells at 50% epiboly (5.5 hpf) in control or MO-*fn1/1b*-injected zebrafish embryos. (**H**) Relative number of *sox17*-GFP^{+} cells at the 9-somite stage (12 hpf) in control or MO- *fn1/1b*-injected zebrafish embryos. (**I**) Sagittal section of control or MO-*fn1/1b* morphant *sox17*-GFP zebrafish embryos at 50% epiboly (5.5 hpf) after *in situ* hybridization for expression of *ntl* (black); immunofluorescence indicates *sox17*-GFP^{+} cells in the *ntl* expression domain after *fn1/1b* knockdown. (**J**) Relative level of *Sox17* mRNA in mES cells co-cultured with control or Fn1-deficient End2 cells. (**K**) Percentage GFP^{+} cells induced in mES$^{Nkx2.5\text{-}GFP}$ cells at day 6 by co-culture with control or Fn1-deficient End2 cells. (**L**) Relative number of Kdr^{+} Pdgfra^{+} precardiac mesoderm cells induced at day 4 by control or Fn1-deficient End2 cells. (**M**) cTnT and DAPI (nuclei) staining of day-8 replated Bry-GFP^{+} mesoderm isolated from co-culture of mES$^{Bry\text{-}GFP}$ cells with control End2 or Fn1-deficient End2 cells at day 4. (**N**) Percentage of cTnT^{+} cells in M quantified by FACS. (**O**) Dorsal views of *gata5* expression in zebrafish embryos at the 10-somite stage, assayed by *in situ* hybridization after control or *fn1/1b* knockdown. pcm, pre-cardiac mesoderm; lpm, lateral plate mesoderm. (**P**) Dorsal views of *myl7* expression in zebrafish embryos at the 16-somite stage, assayed by *in situ* hybridization after control or *fn1/1b* knockdown. Cardiac progenitors are indicated by arrows. *P<0.05, n≥5. Error bars indicate s.e. of biological replicates. KD, knockdown.

Loss of Fn1 has been linked to cardiac as well as generalized mesodermal defects *in vivo*, but the phenotypes are thought to arise much later and be secondary to structural and migratory defects, such as failure to form cadherin junctions as well as mislocalized atypical protein kinase C (aPKC). To examine whether these structural defects could account for the decrease in Bry$^+$ cells, we immunostained for cadherins and aPKC in End2 cells or in End2 cell-containing EBs treated with *fn1* siRNA or control siRNA. The presence or absence of Fn1 did not alter the ability of End2 cells to form cadherin junctions or alter aPKC localization (supplementary material Fig. S2E-G) Furthermore, in EBs containing End2 cells with reduced Fn1 levels, we observed no increase in cell death, no decrease in mesoderm proliferation, nor any increase in expression of pluripotency genes (supplementary material Fig. S2H-J). To examine whether knockdown of Fn1 affected any other ECM components, we compared expression of various ECM components in *fn1* siRNA-treated cells with control-treated cells using ECM-specific gene expression arrays. *Fn1* was the only ECM gene that was significantly downregulated by more than twofold in End2 cells and EBs expressing *fn1* siRNAs (supplementary material Fig. S2K), further confirming the specificity of our knockdown and its effects. These data suggest that Fn1 might play a direct signaling role during the emergence of mesoderm.

To investigate whether fibronectin also promotes the formation of Bry$^+$ cells *in vivo*, we knocked down fibronectin in zebrafish embryos by injecting a morpholino-modified antisense oligonucleotide directed against *fn1* and *fn1b* (MO-*fn1/fn1b*) (Jülich et al., 2005), as there are two fibronectin genes in zebrafish (Trinh and Stainier, 2004; Jülich et al., 2005). As described previously (Jülich et al., 2005), the fibronectin morphants had severe defects in somite boundary formation (data not shown), confirming the efficacy and specificity of the oligonucleotides. The resulting morphants showed no obvious developmental delays or perturbation in gastrulation. However, both the expression level and domain of the zebrafish *Bry* ortholog *no tail* (*ntl*) were markedly decreased at 50% epiboly, a stage equivalent to mid-gastrulation in mouse (Fig. 3D). Expression of *goosecoid* (*gsc*), another mesodermal gene, was similarly decreased at late gastrulation (90% epiboly) (Fig. 3E). At this stage, the decrease in the expression domain of *ntl* was less apparent, suggesting partial late recovery (supplementary material Fig. S2L).

Given that early mesoderm is derived from mesendodermal progenitors (Rodaway and Patient, 2001), we tested whether the loss of fibronectin also affected endodermal cells *in vivo*. We injected MO-*fn1/fn1b* into transgenic zebrafish embryos expressing GFP under control of the *sox17* promoter to label endodermal cell populations (Sakaguchi et al., 2006). The knockdown of *fn1/fn1b* resulted in expansion of the *sox17*-GFP expression domain at mid-gastrulation (50% epiboly) (Fig. 3F). Consistently, the number of GFP$^+$ cells was greatly increased in *fn1/1b* morphants (Fig. 3F,G). Double labeling of cells for *ntl* revealed the abnormal presence of *sox17*-GFP$^+$ cells within the expected *ntl* expression domain (Fig. 3I). Six hours later, at the 9-somite stage [~12 hours postfertilization (hpf)], the expanded population of *sox17*-GFP$^+$ cells in the morphants followed a stereotypical endodermal migration and merged at the midline; however, the overabundance of *sox17*-GFP$^+$ cells was less dramatic at this point (Fig. 3F,H). In agreement, numerous endodermal genes were upregulated in mouse EBs formed in Fn1-deficient End2-ES cell co-culture (Fig. 3J; supplementary material Fig. S3A). These results might reflect an early expansion of endoderm at the expense of mesoderm and are consistent with fibronectin playing a role in normal mesodermal cell fate specification.

Loss of fibronectin negatively affects precardiac mesoderm

Loss of fibronectin results in cardiac defects in both mouse and zebrafish, presumably as a consequence of cell migration abnormalities (George et al., 1993; Trinh and Stainier, 2004). To determine whether fibronectin is also involved in an earlier process – the proper emergence of cardiac progenitors – we performed siRNA knockdown of Fn1 in End2 cells and in those co-cultured with mES$^{Nkx2.5\text{-}GFP}$ cells. Depleting Fn1 in End2 cells significantly reduced the number of Nkx2.5-GFP$^+$ cardiac progenitors by day 5 of differentiation (Fig. 3K).

We investigated whether the decrease in Nkx2.5-GFP$^+$ progenitors was due to a general loss of mesoderm or to a specific loss of precardiac mesoderm. Bry-GFP$^+$ cells were induced by End2 cells treated with control or *fn1* siRNA, and the percentage of precardiac mesodermal cells, identified by co-expression of the surface markers Kdr and Pdgfrα (Kattman et al., 2011), was analyzed among the resulting Bry-GFP$^+$ cell populations by FACS. The number of Kdr$^+$ Pdgfrα$^+$ cells was reduced by 60% (from 25% to 11% of cells) in the Bry-GFP$^+$ cell population exposed to Fn1-deficient End2 cells (Fig. 3L). In agreement with this reduction, the Bry-GFP$^+$ cell population isolated from Fn1-deficient End2 cells differentiated poorly into cardiomyocytes (cTnT$^+$ cells) under differentiation conditions favoring the cardiac lineage (Fig. 3M,N; see Materials and methods). When sorted Bry-GFP$^+$ cells were differentiated in a non-biased manner, we observed a decrease in several mesoderm derivatives, although the cardiac lineage was most adversely affected (supplementary material Fig. S3B).

These data show that decreased levels of endodermal fibronectin result in fewer mesodermal cells and in a disproportionally smaller fraction of precardiac mesoderm. Similarly, in fibronectin-deficient zebrafish embryos, we observed a reduction in cardiac progenitors, as indicated by a decrease in *gata5*$^+$ cardiac primordia at the 10-somite stage, as well as a reduction of the *myosin light chain 7* (*myl7*)$^+$ cardiac domain at the 16-somite stage (Fig. 3O,P). These results suggest that fibronectin promotes the emergence of Bry$^+$ mesoderm and biases toward the formation of precardiac mesoderm.

Fibronectin 1/integrin-β1/β-catenin signaling promotes the emergence of mesoderm

Integrins often play a crucial role in outside-in signaling mediated by ECM proteins (Ieda et al., 2009). Since integrin-β1 is known to mediate fibronectin signaling (Vuori and Ruoslahti, 1993), we disrupted the Fn1–integrin-β1 interaction by treating mES cells with integrin-β1-blocking antibodies (Ieda et al., 2009). This treatment efficiently inhibited the ability of End2 cells to induce Bry-GFP$^+$ mesoderm, similar to that of anti-Fn1 antibodies (Fig. 4A). Correspondingly, End2 cells were less effective in increasing the number of Bry-GFP$^+$ cells in mES cells expressing a dominant-negative form of integrin-β1 (supplementary material Fig. S3C), which affects cell signaling but not cell adhesion or cytoskeletal organization (Ross et al., 1998; Ieda et al., 2009). Combined knockdown of Fn1 and Col4a, the second most differentially expressed ECM protein in End2 cells, resulted in a further decrease in Bry-GFP$^+$ cells (supplementary material Fig. S3D). Similarly, ES cell-specific knockdown of the key integrin signaling component integrin-linked kinase (Ilk) decreased the number of Bry-GFP$^+$ cells in End2 co-culture (supplementary material Fig. S3E). Furthermore, the number of Bry-GFP$^+$ cells was modestly increased when End2 cells were replaced with mouse embryonic fibroblasts (MEFs), which express moderate levels of *fn1* (supplementary material Fig. S3F,G). These results suggest that direct integrin-β1 activation by

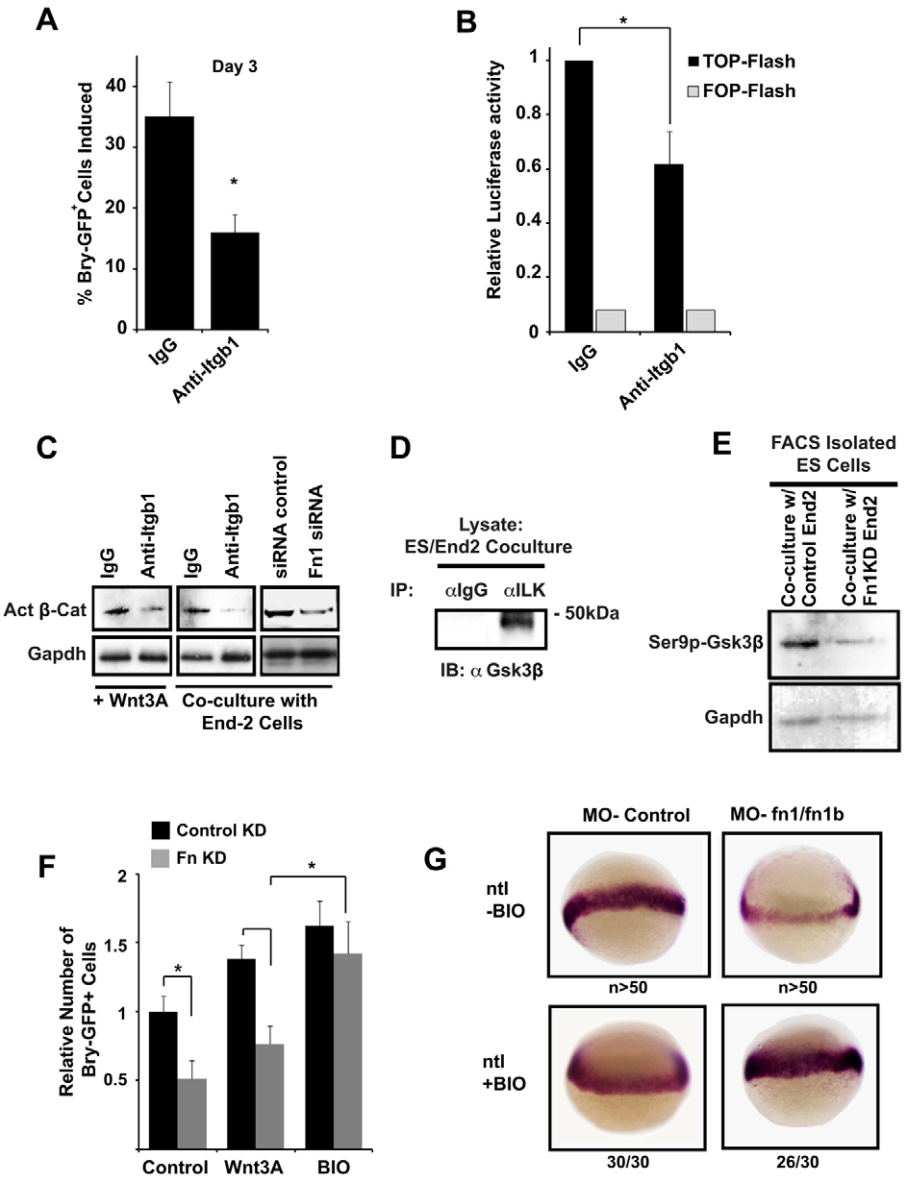

Fig. 4. Fibronectin augments mesoderm induction through integrin-dependent activation of Wnt/β-catenin signaling. (**A**) Percentage of Bry-GFP$^+$ cells induced in day-4 mouse EBs cultured with control (IgG) or anti-integrin-β1 (Itgb1) antibody. (**B**) Relative luciferase activity from a β-catenin/TCF-responsive luciferase construct (TOP-flash) in day-3 EBs with IgG or anti-Itgb1 antibody. The FOP-flash luciferase reporter has a mutation in the TCF binding site. (**C**) Western analysis for active β-catenin in day-3 EBs exposed to Wnt3a or End2 co-culture in the presence or absence of integrin inhibition with anti-Itgb1 or Fn1 knockdown. (**D**) Co-immunoprecipitation (IP) of mES cell/End2 co-culture lysate with control or anti-Ilk antibody immunoblotted (IB) with anti-Gsk3β antibody. (**E**) Western analysis for Ser9-phosphorylated Gsk3β in GFP$^+$ cells sorted from day-3 mES$^{CAG\text{-}GFP}$ cells co-cultured with control or Fn1-deficient End2 cells. (**F**) Relative number of Bry-GFP$^+$ mesoderm cells induced by control or Fn1-deficient End2 cells, with or without Wnt3a or the Wnt agonist BIO. (**G**) *In situ* hybridization for *ntl* expression in zebrafish embryos deficient in *fn1* and *fn1b* (MO-*fn1/fn1b*) at mid-gastrulation (dorsolateral view, animal pole to the top). The *ntl* expression domain was rescued by activation of Wnt signaling via addition of BIO (0.5 μM) to egg water at 2.5 hpf. The number of observed morphant embryos exhibiting displayed phenotype is indicated. *P<0.05, n≥5. Error bars indicate s.e.m. of biological replicates.

fibronectin promotes the emergence of mesoderm, probably along with other secreted proteins.

During somitogenesis, integrin-β1 activates Wnt/β-catenin signaling by phosphorylating and inactivating Gsk3β, resulting in accumulation of the active form of the transcriptional mediator β-catenin (Rallis et al., 2010). We tested whether an analogous integrin-β1-dependent cascade could affect Wnt/β-catenin signaling in mesendodermal cells and thereby the emergence of Bry$^+$ mesodermal cells. Indeed, Bry-GFP$^+$ cells were induced in a Wnt dose-dependent manner in our system (supplementary material Fig. S3H). Introduction of integrin-β1-blocking antibodies decreased the levels of active β-catenin protein and β-catenin/TCF-dependent transcriptional activity (TOP-flash) (Veeman et al., 2003) in Wnt3a-treated differentiating mES cells (Fig. 4B,C). ES cells cultured on exogenous Fn1 also showed higher TOP-flash activity than those cultured on poly-D-lysine (supplementary material Fig. S3I). Similarly, FACS-isolated mES$^{CAG\text{-}GFP}$ cells co-cultured with End2 cells showed decreased levels of active β-catenin in the presence of integrin-β1-blocking antibodies (Fig. 4C). Importantly, knockdown of Fn1 also decreased the End2 cell-responsive accumulation of active β-catenin in sorted mES cells (Fig. 4C), suggesting that Fn1/integrin-β1 signals to positively regulate active β-catenin levels.

Since activated integrin can negatively regulate Gsk3β activity through Ser9 phosphorylation during somitogenesis (Rallis et al., 2010), we investigated whether the Fn1/integrin-β1/β-catenin effect in the mesoderm involved this residue of Gsk3β. We found that Gsk3β co-immunoprecipitated with Ilk, a key signaling component of integrin activation (Fig. 4D). Immunoblotting with an antibody specific for phosphorylated Gsk3β revealed diminished Ser9p-Gsk3β upon non-cell-autonomous decrease in fibronectin (Fig. 4E). Consistent with the epistatic relationship of this model, addition of the Gsk3β inhibitor BIO at day 2 of differentiation to mES cells co-cultured with Fn1-deficient End2 cells rescued the *Bry* induction defects caused by Fn1 knockdown (Fig. 4F). Addition of soluble Wnt3a, which acts upstream of Gsk3β, increased the absolute number of Bry$^+$ cells but could not rescue the relative defect in induction upon Fn1 knockdown (Fig. 4F). Importantly, in zebrafish we observed that the expression domain of *ntl* was restored *in vivo*

when BIO was added to fibronectin morphants at 2.5 hpf, whereas BIO had no significant effect on the *ntl* expression domain in control fish (Fig. 4G).

Together, these results suggest that the endoderm positively regulates mesoderm formation through a fibronectin/integrin-β1/β-catenin signaling cascade.

DISCUSSION

In this study, we demonstrate a previously unrecognized function of endoderm in the development of mesoderm that involves the ECM component fibronectin. Although secreted signals are the predominant morphogens during early development, we demonstrate that ECM components can also play important roles in modulating cell fate decisions. We found that fibronectin signals through integrin-β1 and stimulates Wnt/β-catenin signaling to promote the mesodermal fate, with a specific bias toward precardiac mesoderm. Knockdown of fibronectin resulted in impaired mesoderm induction both *in vitro* and *in vivo* and could be rescued by activating β-catenin signaling intracellularly. These findings address a fundamental aspect of developmental biology regarding cell-cell interactions during early specification.

Fibronectin regulation of endoderm versus mesoderm cell fate

In vivo, fibronectin has a crucial role during early development (George et al., 1993; Jülich et al., 2005). The reported defects upon loss-of-function suggest a structural role for fibronectin. In zebrafish, for example, disruption of the fibronectin-integrin interaction ablates somite boundary formation (Jülich et al., 2005) and causes cardiac bifida with impaired epithelial organization (Trinh and Stainier, 2004). In addition to the structural role, we found that fibronectin is necessary to adequately specify the domains of mesoderm and endoderm during gastrulation, suggesting a morphogenic role of fibronectin.

It is worth noting that fibronectin deficiency reduced expression of the mesendodermal gene *bry* through mid-gastrulation, but the reduction was largely rescued by late gastrulation, probably through a compensatory mechanism. This is consistent with the reported presence of precardiac mesoderm in zebrafish fibronectin morphants, although mesoderm markers were not examined at earlier stages and quantitative measurement of cardiac progenitors was not reported (Trinh and Stainier, 2004). Similarly, earlier reports of fibronectin deletion in mice revealed apparently normal *Bry* expression at the time points examined; however, morphological distortions in mesoderm derivatives were seen as early as E8.0, and thinning of the myocardium was apparent by E9.5 (George et al., 1993; Georges-Labouesse et al., 1996). The persistently abnormal expression of the mesodermal gene *gsc* in our model suggests an incomplete rescue of mesoderm and is in agreement with the more subtle defects in mesoderm derivatives despite the presence of Bry^+ cells.

Contact-mediated signaling during early specification

Our findings may address an interesting conundrum in evolutionary developmental biology. Morphogenesis during development is thought to be governed by conserved three-dimensional signal gradients. However, events prior to organogenesis vary widely in both shape and motion from one species to another. Although the gastrula differ in their shape, the effect of the signal gradients that induce and specify mesoderm, such as Wnt, FGF, Nodal and BMP, is highly conserved (Kimelman et al., 1992; Mercola et al., 2011).

A unifying explanation of this phenomenon might be the existence of a non-diffusible, yet conserved, regulator of gastrulation that signals independently of the three-dimensional structure and signal gradient. It is interesting to note that, in spite of the different gastrulating motions and architectures across vertebrates, initiation of mesoderm always occurs adjacent to endoderm. The fibronectin matrix between endoderm and mesoderm is conserved from mammals to sea urchins (Spiegel et al., 1980). Also conserved is the manner in which gastrulating mesoderm migrates through the secreted fibronectin matrix. Such a high degree of conservation, combined with the novel signaling role uncovered in our study, raises the possibility that fibronectin might be a key mediator of the response of gastrulating cells to diffusible cues in a localized fashion.

An interesting question raised by this study is the specificity of fibronectin in its signaling role. Although integrin-α5β1 is thought to be the primary receptor of fibronectin, mice lacking integrin-α5 have less severe developmental defects than those lacking fibronectin (Yang et al., 1993). This is frequently explained by the ability of ECM components to activate multiple integrin dimers. Complete loss of integrin-β1 signaling results in lethality as early as E6.5 (Chen et al., 2006). The observation that zebrafish fibronectin morphants initiate gastrulation normally implies that integrins are at least partially activated despite fibronectin knockdown. Redundant mechanisms of integrin activation might explain the partial rescue of *ntl* expression in our model. However, the rescue remains incomplete, as evidenced by the persistence of endoderm expansion and other mesodermal defects, including the decrease in *gsc* expression and disproportional loss of cardiac progenitors *in vitro* and *in vivo* (Trinh and Stainier, 2004). The integrin signaling that is involved in normal gastrulation movement therefore appears to be distinct from that involved in the specification and determination of mesoderm. The source of this specificity warrants further study.

ECM-mediated activation of Wnt and Bry

We demonstrated that the fibronectin-integrin interaction promotes mesoderm formation at least in part through Wnt signaling. The decrease in mesoderm upon disruption of fibronectin-integrin interaction was rescued by exogenous inhibition of Gsk3β activity. These findings are consistent with previous observations in somites, where integrin-β1 acts upstream of Wnt signaling and activates Wnt signaling through phosphorylation-dependent inactivation of Gsk3β (Rallis et al., 2010). Although modulation of Wnt signaling can explain the earliest observed defect in Bry induction, it is unlikely to account for all the observed downstream defects. Secondary insults that result from alterations in cell polarization, such as have been observed in earlier studies in zebrafish (Trinh and Stainier, 2004) and *Ciona* (Cooley et al., 2011), are most likely to be important for later specification events that contribute to the complex phenotype observed.

Wnt/β-catenin signaling has biphasic roles during cardiac development. Early activation of Wnt/β-catenin signaling directly regulates *Bry* expression (Yamaguchi et al., 1999) and is required for mesoderm formation (Lindsley et al., 2006), whereas Wnt signaling suppresses the initial induction of $Nkx2.5^+$ cardiac progenitors before positively regulating further expansion of cardiac progenitors (Kwon et al., 2007; Qyang et al., 2007; Ueno et al., 2007; Kwon et al., 2009). This is consistent with the biphasic role of fibronectin observed in our study. Interestingly, Wnt/β-catenin signaling has been reported to regulate the expression of ECM components, including fibronectin (Gradl et al., 1999). This suggests a potential positive-feedback loop for activation and

propagation of Wnt signaling. It will be interesting to determine whether such ECM-mediated spatial localization of the signal response is employed more widely in cell specification during development and adulthood.

Acknowledgements
We thank G. Keller for ES$^{Bry\text{-}GFP}$ cells; C. Mummery for End2 cells; D. Stainier for transgenic Sox17-GFP zebrafish and use of the zebrafish facility; R. Ross for Tacβ1 constructs; K. Tomoda for mouse embryo sections; members of the D.S. and C.K. laboratories for thoughtful discussions; S. Elmes from the UCSF Flow Core for cell sorting; G. Howard and S. Ordway for editorial assistance; B. Taylor for assistance with manuscript and figure preparation; and B. Bruneau for critical reading of the manuscript.

Funding
D.S. was supported by grants from the National Institutes of Health/National Heart, Lung, and Blood Institute (NIH/NHLBI) [U01 HL100406, R01 HL057181, P01 HL089707]; the California Institute for Regenerative Medicine; the William Younger Family Foundation; the L.K. Whittier Foundation; and the Eugene Roddenberry Foundation. C.K. was supported by grants from NIH/NHLBI [R00 HL092234, R01 HL111198]; Maryland Stem Cell Research Fund; and Magic That Matters Fund. P.A. was supported by the Lundbeck Foundation [R83-A8133]. P.C. was supported by an NIH/National Institute of General Medical Sciences (NIGMS) grant [T32 GM07618] to the UCSF Medical Scientist Training Program. This work was supported by an NIH/National Center for Research Resources (NCRR) grant [C06 RR018928] to the Gladstone Institutes. Deposited in PMC for release after 12 months.

Competing interests statement
The authors declare no competing financial interests.

Supplementary material
Supplementary material available online at
http://dev.biologists.org/lookup/suppl/doi:10.1242/dev.089052/-/DC1

References

Buckingham, M., Meilhac, S. and Zaffran, S. (2005). Building the mammalian heart from two sources of myocardial cells. *Nat. Rev. Genet.* **6**, 826-835.
Chen, H., Zou, Z., Sarratt, K. L., Zhou, D., Zhang, M., Sebzda, E., Hammer, D. A. and Kahn, M. L. (2006). In vivo beta1 integrin function requires phosphorylation-independent regulation by cytoplasmic tyrosines. *Genes Dev.* **20**, 927-932.
Cooley, J., Whitaker, S., Sweeney, S., Fraser, S. and Davidson, B. (2011). Cytoskeletal polarity mediates localized induction of the heart progenitor lineage. *Nat. Cell Biol.* **13**, 952-957.
Fehling, H. J., Lacaud, G., Kubo, A., Kennedy, M., Robertson, S., Keller, G. and Kouskoff, V. (2003). Tracking mesoderm induction and its specification to the hemangioblast during embryonic stem cell differentiation. *Development* **130**, 4217-4227.
Fish, J. E., Santoro, M. M., Morton, S. U., Yu, S., Yeh, R. F., Wythe, J. D., Ivey, K. N., Bruneau, B. G., Stainier, D. Y. and Srivastava, D. (2008). miR-126 regulates angiogenic signaling and vascular integrity. *Dev. Cell* **15**, 272-284.
Freund, C., Ward-van Oostwaard, D., Monshouwer-Kloots, J., van den Brink, S., van Rooijen, M., Xu, X., Zweigerdt, R., Mummery, C. and Passier, R. (2008). Insulin redirects differentiation from cardiogenic mesoderm and endoderm to neuroectoderm in differentiating human embryonic stem cells. *Stem Cells* **26**, 724-733.
George, E. L., Georges-Labouesse, E. N., Patel-King, R. S., Rayburn, H. and Hynes, R. O. (1993). Defects in mesoderm, neural tube and vascular development in mouse embryos lacking fibronectin. *Development* **119**, 1079-1091.
Georges-Labouesse, E. N., George, E. L., Rayburn, H. and Hynes, R. O. (1996). Mesodermal development in mouse embryos mutant for fibronectin. *Dev. Dyn.* **207**, 145-156.
Gradl, D., Kühl, M. and Wedlich, D. (1999). The Wnt/Wg signal transducer beta-catenin controls fibronectin expression. *Mol. Cell. Biol.* **19**, 5576-5587.
Hansson, M., Olesen, D. R., Peterslund, J. M., Engberg, N., Kahn, M., Winzi, M., Klein, T., Maddox-Hyttel, P. and Serup, P. (2009). A late requirement for Wnt and FGF signaling during activin-induced formation of foregut endoderm from mouse embryonic stem cells. *Dev. Biol.* **330**, 286-304.
Holtzinger, A., Rosenfeld, G. E. and Evans, T. (2010). Gata4 directs development of cardiac-inducing endoderm from ES cells. *Dev. Biol.* **337**, 63-73.
Hsiao, E. C., Yoshinaga, Y., Nguyen, T. D., Musone, S. L., Kim, J. E., Swinton, P., Espineda, I., Manalac, C., deJong, P. J. and Conklin, B. R. (2008). Marking embryonic stem cells with a 2A self-cleaving peptide: a NKX2-5 emerald GFP BAC reporter. *PLoS ONE* **3**, e2532.
Ieda, M., Tsuchihashi, T., Ivey, K. N., Ross, R. S., Hong, T. T., Shaw, R. M. and Srivastava, D. (2009). Cardiac fibroblasts regulate myocardial proliferation through beta1 integrin signaling. *Dev. Cell* **16**, 233-244.
Inman, K. E. and Downs, K. M. (2006). Localization of Brachyury (T) in embryonic and extraembryonic tissues during mouse gastrulation. *Gene Expr. Patterns* **6**, 783-793.
Jülich, D., Geisler, R., Tübingen 2000 Screen Consortium and Holley, S. A. (2005). Integrinalpha5 and delta/notch signaling have complementary spatiotemporal requirements during zebrafish somitogenesis. *Dev. Cell* **8**, 575-586.
Kattman, S. J., Huber, T. L. and Keller, G. M. (2006). Multipotent flk-1+ cardiovascular progenitor cells give rise to the cardiomyocyte, endothelial, and vascular smooth muscle lineages. *Dev. Cell* **11**, 723-732.
Kattman, S. J., Witty, A. D., Gagliardi, M., Dubois, N. C., Niapour, M., Hotta, A., Ellis, J. and Keller, G. (2011). Stage-specific optimization of activin/nodal and BMP signaling promotes cardiac differentiation of mouse and human pluripotent stem cell lines. *Cell Stem Cell* **8**, 228-240.
Kimelman, D., Christian, J. L. and Moon, R. T. (1992). Synergistic principles of development: overlapping patterning systems in Xenopus mesoderm induction. *Development* **116**, 1-9.
Kimmel, C. B., Ballard, W. W., Kimmel, S. R., Ullmann, B. and Schilling, T. F. (1995). Stages of embryonic development of the zebrafish. *Dev. Dyn.* **203**, 253-310.
Kispert, A. and Herrmann, B. G. (1994). Immunohistochemical analysis of the Brachyury protein in wild-type and mutant mouse embryos. *Dev. Biol.* **161**, 179-193.
Kitajima, S., Takagi, A., Inoue, T. and Saga, Y. (2000). MesP1 and MesP2 are essential for the development of cardiac mesoderm. *Development* **127**, 3215-3226.
Kwon, C., Arnold, J., Hsiao, E. C., Taketo, M. M., Conklin, B. R. and Srivastava, D. (2007). Canonical Wnt signaling is a positive regulator of mammalian cardiac progenitors. *Proc. Natl. Acad. Sci. USA* **104**, 10894-10899.
Kwon, C., Qian, L., Cheng, P., Nigam, V., Arnold, J. and Srivastava, D. (2009). A regulatory pathway involving Notch1/beta-catenin/Isl1 determines cardiac progenitor cell fate. *Nat. Cell Biol.* **11**, 951-957.
Lindsley, R. C., Gill, J. G., Kyba, M., Murphy, T. L. and Murphy, K. M. (2006). Canonical Wnt signaling is required for development of embryonic stem cell-derived mesoderm. *Development* **133**, 3787-3796.
Liu, Y., Asakura, M., Inoue, H., Nakamura, T., Sano, M., Niu, Z., Chen, M., Schwartz, R. J. and Schneider, M. D. (2007). Sox17 is essential for the specification of cardiac mesoderm in embryonic stem cells. *Proc. Natl. Acad. Sci. USA* **104**, 3859-3864.
Marvin, M. J., Di Rocco, G., Gardiner, A., Bush, S. M. and Lassar, A. B. (2001). Inhibition of Wnt activity induces heart formation from posterior mesoderm. *Genes Dev.* **15**, 316-327.
Mercola, M., Ruiz-Lozano, P. and Schneider, M. D. (2011). Cardiac muscle regeneration: lessons from development. *Genes Dev.* **25**, 299-309.
Mummery, C., Ward-van Oostwaard, D., Doevendans, P., Spijker, R., van den Brink, S., Hassink, R., van der Heyden, M., Opthof, T., Pera, M., de la Riviere, A. B. et al. (2003). Differentiation of human embryonic stem cells to cardiomyocytes: role of coculture with visceral endoderm-like cells. *Circulation* **107**, 2733-2740.
Murry, C. E. and Keller, G. (2008). Differentiation of embryonic stem cells to clinically relevant populations: lessons from embryonic development. *Cell* **132**, 661-680.
Nijmeijer, R. M., Leeuwis, J. W., DeLisio, A., Mummery, C. L. and Chuva de Sousa Lopes, S. M. (2009). Visceral endoderm induces specification of cardiomyocytes in mice. *Stem Cell Res. (Amst.)* **3**, 170-178.
Qyang, Y., Martin-Puig, S., Chiravuri, M., Chen, S., Xu, H., Bu, L., Jiang, X., Lin, L., Granger, A., Moretti, A. et al. (2007). The renewal and differentiation of Isl1+ cardiovascular progenitors are controlled by a Wnt/beta-catenin pathway. *Cell Stem Cell* **1**, 165-179.
Rallis, C., Pinchin, S. M. and Ish-Horowicz, D. (2010). Cell-autonomous integrin control of Wnt and Notch signalling during somitogenesis. *Development* **137**, 3591-3601.
Rodaway, A. and Patient, R. (2001). Mesendoderm. an ancient germ layer? *Cell* **105**, 169-172.
Ross, R. S., Pham, C., Shai, S. Y., Goldhaber, J. I., Fenczik, C., Glembotski, C. C., Ginsberg, M. H. and Loftus, J. C. (1998). Beta1 integrins participate in the hypertrophic response of rat ventricular myocytes. *Circ. Res.* **82**, 1160-1172.
Rudy-Reil, D. and Lough, J. (2004). Avian precardiac endoderm/mesoderm induces cardiac myocyte differentiation in murine embryonic stem cells. *Circ. Res.* **94**, e107-e116.
Sakaguchi, T., Kikuchi, Y., Kuroiwa, A., Takeda, H. and Stainier, D. Y. (2006). The yolk syncytial layer regulates myocardial migration by influencing extracellular matrix assembly in zebrafish. *Development* **133**, 4063-4072.
Schultheiss, T. M. and Lassar, A. B. (1997). Induction of chick cardiac myogenesis by bone morphogenetic proteins. *Cold Spring Harb. Symp. Quant. Biol.* **62**, 413-419.

Schultheiss, T. M., Xydas, S. and Lassar, A. B. (1995). Induction of avian cardiac myogenesis by anterior endoderm. *Development* **121**, 4203-4214.
Spiegel, E., Burger, M. and Spiegel, M. (1980). Fibronectin in the developing sea urchin embryo. *J. Cell Biol.* **87**, 309-313.
Srivastava, D. (2006). Making or breaking the heart: from lineage determination to morphogenesis. *Cell* **126**, 1037-1048.
Trinh, L. A. and Stainier, D. Y. (2004). Fibronectin regulates epithelial organization during myocardial migration in zebrafish. *Dev. Cell* **6**, 371-382.
Ueno, S., Weidinger, G., Osugi, T., Kohn, A. D., Golob, J. L., Pabon, L., Reinecke, H., Moon, R. T. and Murry, C. E. (2007). Biphasic role for Wnt/beta-catenin signaling in cardiac specification in zebrafish and embryonic stem cells. *Proc. Natl. Acad. Sci. USA* **104**, 9685-9690.
Veeman, M. T., Slusarski, D. C., Kaykas, A., Louie, S. H. and Moon, R. T. (2003). Zebrafish prickle, a modulator of noncanonical Wnt/Fz signaling, regulates gastrulation movements. *Curr. Biol.* **13**, 680-685.
Vuori, K. and Ruoslahti, E. (1993). Activation of protein kinase C precedes alpha 5 beta 1 integrin-mediated cell spreading on fibronectin. *J. Biol. Chem.* **268**, 21459-21462.
Westerfield, M. (1995). *The Zebrafish Book. A Guide for the Laboratory Use of Zebrafish (Danio rerio)*. Eugene, OR: University of Oregon Press.
Wilkinson, D. G., Bhatt, S. and Herrmann, B. G. (1990). Expression pattern of the mouse T gene and its role in mesoderm formation. *Nature* **343**, 657-659.
Yamaguchi, T. P., Takada, S., Yoshikawa, Y., Wu, N. and McMahon, A. P. (1999). T (Brachyury) is a direct target of Wnt3a during paraxial mesoderm specification. *Genes Dev.* **13**, 3185-3190.
Yang, J. T., Rayburn, H. and Hynes, R. O. (1993). Embryonic mesodermal defects in alpha 5 integrin-deficient mice. *Development* **119**, 1093-1105.
Yang, L., Soonpaa, M. H., Adler, E. D., Roepke, T. K., Kattman, S. J., Kennedy, M., Henckaerts, E., Bonham, K., Abbott, G. W., Linden, R. M. et al. (2008). Human cardiovascular progenitor cells develop from a KDR+ embryonic-stem-cell-derived population. *Nature* **453**, 524-528.

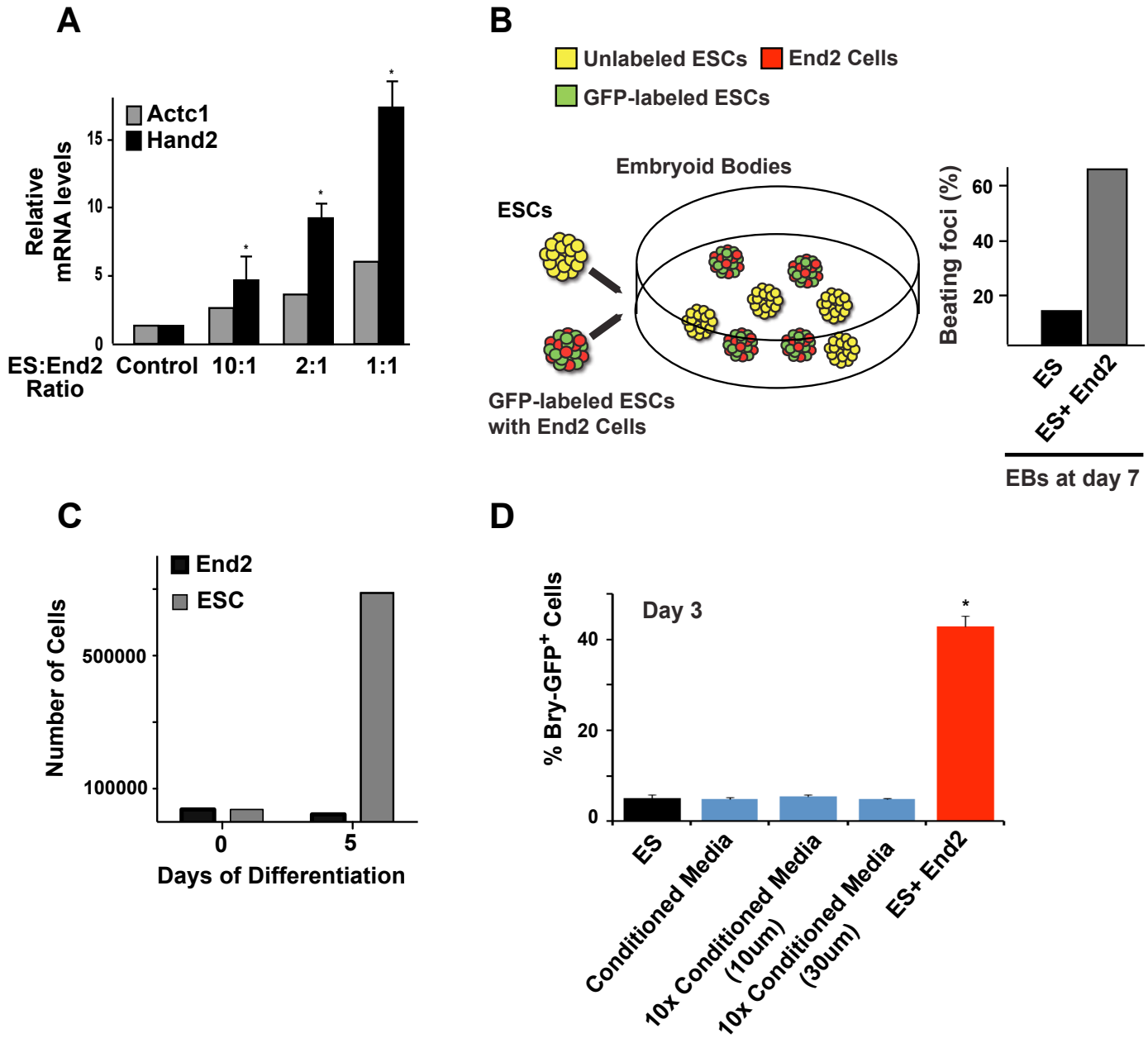

Fig. S1. Endoderm-like (End2) cells promote the emergence of mesoderm in ES cells through a short-range signal. (**A**) Relative expression of cardiac genes *Actc1* and *Hand2* in embryoid bodies (EBs) formed with increasing ratios of End2 cells relative to mES cells (ESCs). (**B**) Percentage of beating foci observed in a mixed culture of EBs formed with (green/red) or without (yellow) End2 cells. (**C**) Number of mES cells and End2 cells at day 0 and after 5 days of co-culture. (**D**) Percentage of Bry-GFP^{+} mesodermal cells in EBs differentiated with End2 cells, End2-conditioned medium, or conditioned medium concentrated via a 10 or 30 μm filter. **P*<0.05, error bars indicate s.e.m.

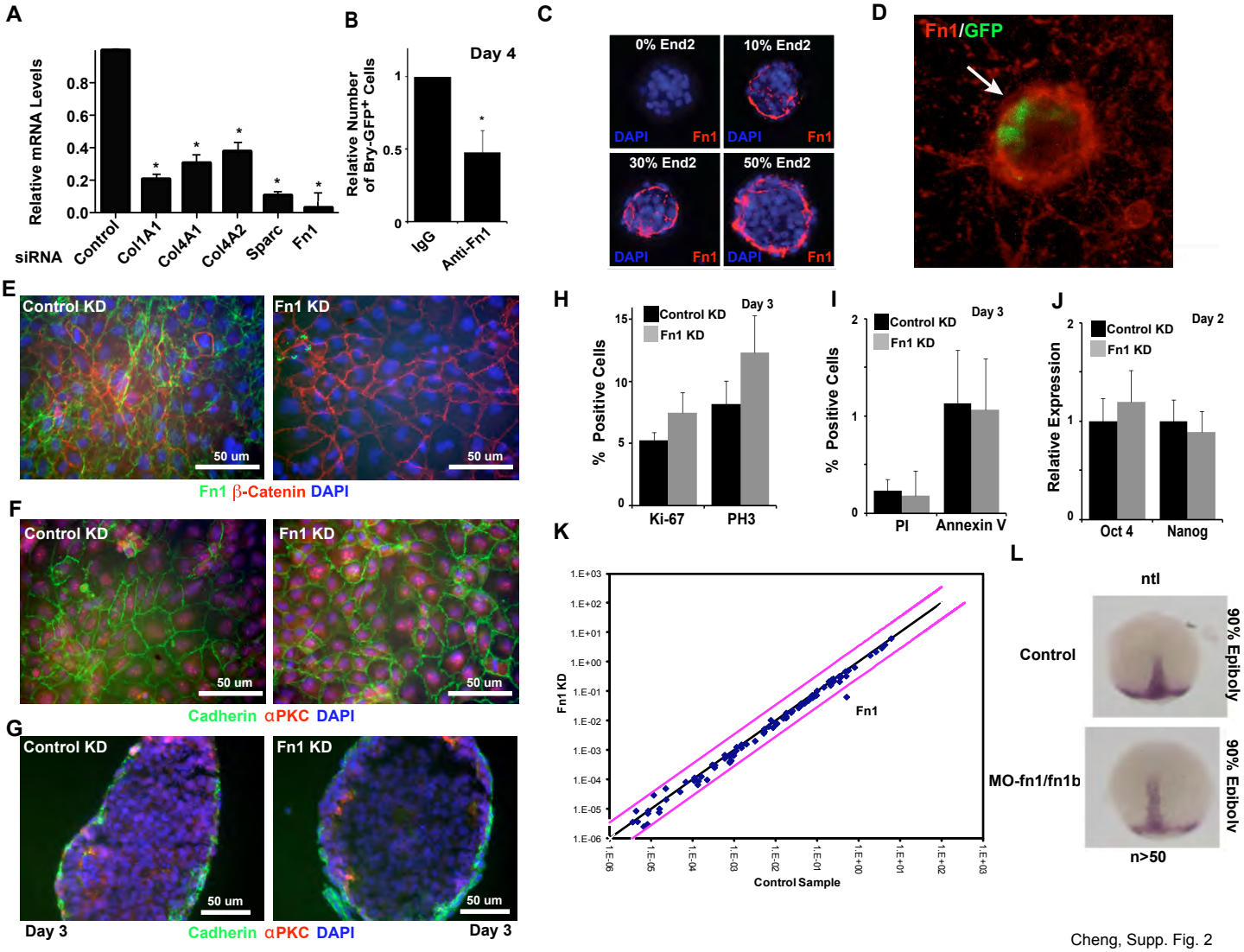

Fig. S2. Fibronectin promotes End2-mediated induction of mesoderm and precardiac mesoderm *in vitro* and *in vivo*. (**A**) Knockdown efficiency of the indicated siRNAs assayed by qPCR. (**B**) Percentage of Bry-GFP$^+$ cells in day-4 EBs cultured with End2 cells with control (IgG) or anti-Fn1 antibody. (**C**) EBs with increasing ratio of End2 cells stained with DAPI and Fn1 antibody. (**D**) Adherent culture of mES$^{Bry\text{-}GFP}$ EBs plated with End2 cells and stained for Fn1 (red) and GFP (green). (**E**) End2 cells 48 hours after transfection with scrambled siRNA or siRNA against Fn1, stained for Fn1 (green) and β-catenin (red). (**F**) End2 cells 48 hours after transfection with scrambled siRNA or siRNA against Fn1, stained for pan-cadherin (green) and aPKC (red). (**G**) EBs containing End2 cells transfected with scrambled siRNA or siRNA against Fn1, stained for pan-cadherin (green) and aPKC (red). (**H**) FACS analysis of cell proliferation as assayed by Ki-67 or phosphohistone H3 (PH3) staining among Bry-GFP$^+$ cells in EBs aggregated with control or fibronectin-deficient End2 cells. (**I**) FACS analysis of cell death as assayed by propidium iodide (PI)$^+$ and annexin V staining among Bry-GFP$^+$ populations in EBs aggregated with control or fibronectin-deficient End2 cells. (**J**) Expression of the pluripotent genes *Oct4* and *Nanog* in day-2 EBs with control or Fn1-deficient End2 cells. (**K**) Scatter plot of ECM mRNA array from EBs co-cultured with control or Fn1 knockdown End2 cells. (**L**) Whole-mount *in situ* hybridization of *ntl* in control or Fn1/Fn3 knockdown (MO-Fn1/3) zebrafish embryos at 90% epiboly (9 hpf). **P*<0.05, error bars indicate s.e.m.

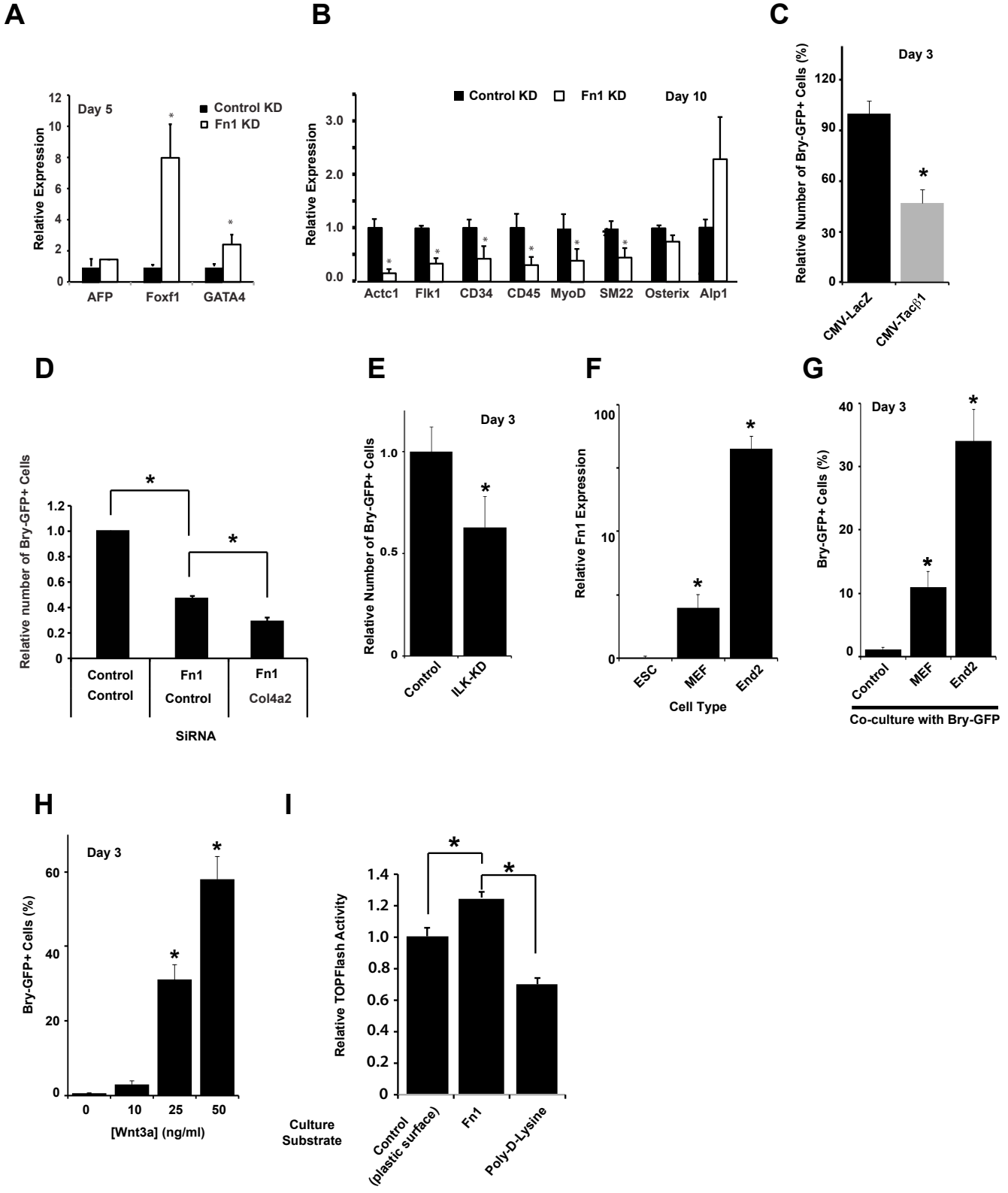

Fig. S3. Fibronectin augments mesoderm induction through integrin-dependent activation of Wnt/β-catenin signaling. (**A**) Expression of various endodermal markers in cells differentiated from Bry-GFP$^+$ cells isolated from EBs with control or Fn1 knockdown (KD). (**B**) Expression of various mesodermal markers in cells differentiated from Bry-GFP$^+$ cells isolated from EBs with control or Fn1-deficient End2 cells. (**C**) Relative number of Bry-GFP$^+$ cells induced by End2 cells in differentiating mES$^{Bry\text{-}GFP}$ cells with overexpression of the integrin signaling mutant Tacβ1 or control (*lacZ*). (**D**) Relative number of Bry-GFP$^+$ cells induced by End2 cells transfected with control and/or Fn1/Col4a2 siRNA. (**E**) Relative number of Bry-GFP$^+$ cells in End2 co-cultures with mES$^{Bry\text{-}GFP}$ cells transfected with control or Ilk siRNA. (**F**) Relative *Fn1* expression in ESCs, MEFs or End2 cells. (**G**) Percentage Bry-GFP$^+$ cells observed in differentiation with ESCs alone, or co-culture with MEFs or End2 cells. (**H**) Percentage Bry-GFP$^+$ cells induced by increasing concentrations of Wnt3a. (**I**) Relative TOP-flash activity in differentiated ESCs cultured on Fn1 or poly-D-lysine. *P<0.05, n=3 or greater. Error bars indicate s.e.m.

Movie 1. Spontaneous contraction of cardiomyocytes differentiated from End2-induced precardiac mesoderm.

Table S1. Expression of ECM genes in End2 cells versus ES and ectodermal cells

Symbol	Log_2 (FC)	*P*-value	Expressed around egg-cylinder and gastrulation stage
Fn1	**2.36832369**	**0.000482225**	**+**
Lama3	−3.69437791	0.004787302	
Col4a1	**5.39362669**	**0.006466226**	**+**
Col4a2	**2.25451884**	**0.009827216**	**+**
Timp3	**4.78813179**	**0.010284841**	**−**
Itgav	1.81114939	0.011167394	
Sparc	**2.88647209**	**0.013530666**	**+**
Cdh2	**2.00801929**	**0.013980868**	**−**
Sgce	**2.51501439**	**0.017630714**	**−**
Ctnnb1	−1.62105666	0.01829935	
Timp2	**4.80258464**	**0.020218724**	**−**
Col1a1	**6.11512519**	**0.020504982**	**+**
Cntn1	−1.52143081	0.021217884	
Thbs3	−1.55693326	0.024294494	
Vcam1	6.87848319	0.028849818	
Adamts5	2.66148604	0.029912537	
Mmp2	2.41154834	0.03266755	
Ctnna2	2.24932944	0.036734739	
Thbs2	−3.59531056	0.041485655	
Col3a1	6.66594809	0.04231551	
Col5a1	1.55671699	0.047171288	
Itgam	−2.18766771	0.052602835	
Tnc	3.28507064	0.05851667	
Itgb1	0.90042484	0.058915566	
Hapln1	−2.41886931	0.063244531	
Cdh3	1.52066139	0.064073183	
Itgb3	4.04664894	0.071629966	
Mmp13	3.58515104	0.072185608	
Cd44	4.93159714	0.081185984	
Pecam1	−5.15819076	0.082377403	
Thbs1	4.53810729	0.084706461	
Postn	2.96244189	0.090221262	
Adamts1	2.73405889	0.099148625	
Spp1	−5.03487621	0.113469299	
Ncam1	0.81139574	0.121124338	
Lamb2	0.73336334	0.135373586	
Itgb4	−1.00554206	0.150664561	
Mmp14	1.39571854	0.155233801	
Col6a1	7.11230019	0.165616311	
Itgal	−2.57583136	0.167756088	
Selp	1.47631989	0.173485089	
Mmp8	2.99186449	0.182355545	
Mmp9	−3.36491961	0.187441341	
Lamb3	−2.97790276	0.191517903	
Sele	1.88041984	0.193782813	

Adamts2	1.15955854	0.203361496
Col4a3	1.39159194	0.209170667
Col2a1	−4.03470811	0.209645434
Cdh1	−4.95819166	0.223356991
Spock1	−3.01631216	0.240265978
Mmp15	−1.47104581	0.240576219
Icam1	−0.11250206	0.243198795
Adamts8	−1.85968281	0.25723376
Mmp11	−0.56176436	0.259450606
Ctgf	0.28752319	0.269014355
Syt1	1.51337214	0.270920915
Emilin1	−2.35108266	0.292417197
Mmp1a	1.29737074	0.300237402
Vcan	1.09386404	0.319549642
Itga3	1.11160969	0.321351939
Ncam2	−1.48765866	0.343283912
Ecm1	0.62412304	0.360233824
Lama2	0.28008739	0.367725047
Mmp7	1.40926059	0.371188088
Itga2	0.90122809	0.376339274
Sell	0.80391174	0.384569169
Tgfbi	−2.19130066	0.394459931
Timp1	−1.43928676	0.40153966
Lama1	−4.47066411	0.408702404
Hc	0.09429884	0.426772266
Mmp12	0.27556214	0.435886078
Ctnna1	−0.05077756	0.53954357
Mmp3	0.61166869	0.543160669
Itgax	0.04080364	0.549823798
Itga5	0.24840284	0.561258646
Lamc1	0.01268754	0.605250367
Itga4	−0.62558746	0.638477331
Itgb2	−0.84664986	0.652115056
Cdh4	−4.15708061	0.744720352
Fbln1	−0.77668296	0.748958051
Itgae	−0.10477356	0.773917062
Mmp10	0.91885374	0.794369608
Entpd1	−0.15355406	0.831367709
Vtn	0.00488484	0.89528792

Cut-offs were set at >4-fold increase, *P*>0.025.